Arabian Journal of Geosciences (2021) 14:400
https://doi.org/10.1007/s12517-021-06727-x

ORIGINAL PAPER

Efficiency of natural clay and titania P25 composites in the decolouring of methylene blue (MB) from aqueous solutions: dual adsorption and photocatalytic processes

Khalil Lazaar[1] · Hajer Chargui[1] · Robert Pullar[2,3] · Walid Hajjaji[4] · Bechir Moussi[1] · João Labrincha[2] · Fernando Rocha[5] · Fakher Jamoussi[1]

Received: 13 February 2020 / Accepted: 16 February 2021

Abstract
In this paper, we use Tunisian clay materials as alternative low-cost adsorbents, as well as substrates to immobilise TiO_2 for the decolouration of methylene blue (MB) dye solutions. The collected raw clay from the mine of Tamra was characterised by various techniques, such as X-ray diffraction (XRD), scanning electron microscopy (SEM) and X-ray fluorescence (XRF). XRD patterns of the raw clay showed halloysite as the main phase (61%), with a lower content of kaolinite (39%). For MB adsorption, the experimental data were fitted by Langmuir and Freundlich adsorption equations. It was found that the studied clays alone were not very efficient at adsorbing MB dye molecules. The decolouration of MB was improved by adding a photocatalytic function to the clay, by adding various amounts of TiO_2 nanopowder (20–80 wt%) to the clay, imbuing it with photocatalytic capabilities. These combined effects of the phenomena of adsorption and photocatalysis for MB removal by the TiO_2-doped clay resulted in a very satisfactory performance, even with the relatively low quantity of 20 wt% added TiO_2 photocatalyst. This gave 48.6% removal after only 30-min adsorption in the dark, increasing to 84.1% removal after a further 3 h under UV light, through combined chemo-physical adsorption and photocatalytic decolouration phenomena.

Keywords Halloysite-rich clay · Titania · Methylene blue · Adsorption · Photocatalysis

Introduction

Dyes are organic compounds which are used in many industries, such as paper, textiles, food processing, cosmetics, pharmaceuticals, and medical diagnostics (Annadurai et al. 2002; Dogan and Alkan 2003; Alahiane et al. 2013). Dye-contaminated wastewater contains coloured compounds from the residues of dyes and various chemical additives (Mahammedi and Benguella 2016). The majority of synthetic textile dyes produced globally (700,000 tons per year) are classified as azo compounds, which contain an N-chromophore molecule, for example, methylene blue ($C_{16}H_{18}N_3SCl$). This is the most commonly used dye in dyeing cotton, silk, and wood. It can cause eye burns that can permanently injure the eyes of man and animals. Inhalation may result in difficulty in breathing, and ingestion produces a burning sensation, and can result in nausea, vomiting, and heavy cold sweats. Dyes in surface waters can also result in other harmful environmental effects, such as blocking the photosynthesis of water borne flora.

The treatment of industrial waste containing this type of dye is of great interest (Sakr et al. 2015; Lazaar et al. 2017), but the removal of low levels of such compounds is difficult. Several methods and techniques have been developed in recent years. These techniques include chemical precipitation

Responsible Editor: Amjad Kallel

✉ Khalil Lazaar
lazaar.khalil@yahoo.fr

[1] Georessources Laboratory, CERTE, 273, 8020 Soliman, Tunisia

[2] Department of Materials and Ceramic Engineering / CICECO – Aveiro Institute of Materials, University of Aveiro, 3810-193 Aveiro, Portugal

[3] Department of Molecular Sciences and Nanosystems (DSMN), Ca' Foscari University of Venice, Scientific Campus, Via Torino 155, 30172 Mestre, VE, Italy

[4] LABTEN Natural Water Treatment Laboratory, CERTE, 273, 8020 Soliman, Tunisia

[5] Geobiotec, Geosciences Department, University of Aveiro, 3810-193 Aveiro, Portugal

Published online: 02 March 2021

process flocculation (Chaari et al. 2015), ion exchange, electrolysis, membrane processes (Das and Basu 2014), and adsorption (Lazaar et al. 2017). The last one is the most common technique for dye removal, as it is easy to implement and is a cost-effective process to remove dyes from aqueous solution, and it has been tested with many adsorbents (Hajjaji et al. 2013).

Several researchers have shown that a wide variety of materials of natural or biological origin have the ability to remove large amounts of organic pollutants from water (Weber et al. 2011; Naidoo and Olaniran 2014; Chakraborty et al. 2014; Das et al. 2014; Bhattacharjee et al. 2014; Sarkar et al. 2015; Chakraborty et al. 2017; Aloulou et al. 2018; Shakeel et al., 2019; Asefi et al. 2019; Ahmedkhan et al. 2019; Priya et al. 2020; Tunç et al. 2019). Activated carbon (Yu-Li and Thomas 1995; Meshko et al. 2001), alumina (Crini 2006), and zeolites (Meshko et al. 2001) are considered some of the most versatile adsorbents, and many studies show their effectiveness, but their use is limited due to difficulties in their regeneration, and their relatively high cost (Sadlki et al. 2014). An alternative solution would be to use other efficient and economic adsorbent materials. We chose a material that is abundant in Tunisia: a clay from the Nefza region of northern Tunisia (Eloussaief et al. 2009; Sdiri et al. 2014).

Clays have been studied for various applications such as adsorption and catalysis (Chaari et al. 2008; Hajjaji et al. 2013; Hajjaji et al. 2016; Mhammedi and Benguella 2016). Clayey mineral was some of natural materials that were successfully used for contaminant removal (Chargui et al. 2018). This approach of natural adsorbents for the treatment of wastewater was the focus of much research in the last decade (Ben Amor et al. 2018). Clayey materials are used commercial adsorbents due to their low cost, abundant availability, easy accessibility, environmentally friendly nature, a large surface area, and their abundance in nature.

This focus on clay minerals is due to their many possible variations in structure, along with chemical stability and high specific surface area (Mudzielwana et al. 2019). Halloysite clays are the most effective adsorbents used in the removal of dyes (Chaari et al. 2015). Halloysite was first described by Berthier (1826) as a dioctahedral 1:1 clay mineral of the kaolin group. However, halloysite often forms a major component of Andisols (soils formed in volcanic ash containing high proportions of glass and amorphous colloidal materials), and other soils derived from volcanic materials in wet tropical and subtropical regions. The structure and chemical composition of halloysite is similar to that of kaolinite, dickite, or nacrite, but the unit layers in halloysite are separated by a monolayer of water molecules. The particles of halloysite can adopt a variety of morphologies, the most common of which is the elongated tubule.

Recent research has demonstrated photocatalytic degradation by titania of both organic and inorganic contaminants in wastewater, and of gaseous pollutants (Ngoh and Nawi 2016). Due to its availability, relative low cost, non-toxicity, thermal and chemical stability, high hydrophilicity, and photoactivity in solar or visible light, titanium dioxide (TiO_2) remains the most studied photocatalyst in the field of environmental treatments (Arana et al. 2002; Mokhbi et al. 2014). Its high specific surface area (nanosized particles) and oxidation ability make it suitable for the decomposition of a wide range of organic pollutants (Wongso et al. 2019).

Heterogeneous photocatalysis, an advanced oxidation photochemical technique, has the advantage of being capable of oxidising numerous water-borne contaminants (fertilisers, pesticides, dyes, pharmaceutical molecules) until they are completely destroyed (mineralisation). However, a major drawback in using titania powders as photocatalysts is their tendency to aggregate/agglomerate, especially when used as a nanopowder, as well as the subsequent removal of this nanomaterial. Agglomeration reduces the surface area and, hence, the photocatalytic efficiency of titania nanopowders (Bhattacharya et al. 2006; Hajjaji et al. 2013). To avoid this problem, trials have focused on developing suitable substrates to immobilise the fine TiO_2 particles (Gong et al. 2015). Among these materials, clayey minerals are a good alternative (Hajjaji et al. 2013; Mustapha et al. 2020). This process is based on the immobilisation of the particles of the photocatalysts, generally TiO_2, on the clay. TiO_2/clay composites have advantages over commercial photocatalysts such as high surface area, high hydrophobicity, and low economic cost.

Therefore, a number of publications have focused on the use of halloysite-rich clay for the removal of various pollutants such as organic and inorganic compounds, heavy metals, and microorganisms. In addition to this, applications of porous materials such as clays have recently been extended to the catalytic oxidation of water pollutants. These materials are used either as active catalyst in itself, or as a supported substrate due to their high surface area (Djebali 2015).

Therefore, in this paper, the potential use of Tunisian clayey deposits is studied, both as an alternative low-cost adsorbent for the treatment of wastewater and as composite materials with added TiO_2 and photocatalytic capabilities to enhance the removal of a cationic dye (methylene blue) from water using combined absorption and photodegradation.

Materials and methods

Materials

The raw halloysite-rich clay (H) was obtained from the northeast Nefza region (northern Tunisia). The TiO_2 used was a commercial titania nanopowder (Aeroxide P25, Evonik). The mixed clay-titania material was prepared by mixing the

raw clay with the commercial titania. Four photocatalyst mixtures, each with a mass of 1 g, were prepared by adding clay to titania with the ratios of TiO_2:clay of 100:0 (Ti, pure titania); 80:20 (Ti80); 50:50 (Ti50); and 20:80 (Ti20). The mixtures were ground for 2 min in an agate mortar. P25 has been well characterised in a previous paper by some of the authors: it is composed of 76.3 wt% anatase, 10.6 wt% rutile, and 13.0 wt% amorphous TiO_2, with an average particle size of 21 nm (Tobaldi et al. 2014).

Physical characterisation

The mineralogical analysis was carried out by X-ray diffraction (XRD, Phillips X'Pert diffractometer equipped with Cu kα radiation) on the total rock and the oriented aggregates, either as a normal slide or after heating for 2 h at 500 °C (resulting in weight loss, destruction of kaolinite, and displacement of basal reflection (001) for other clay minerals) (Hajjaji 2011), with ethylene glycol. The chemical composition of powdered samples was measured by X-ray fluorescence (XRF, Panalytical Axios Dispersive X-ray Fluorescence Spectrometer). The morphology was characterised by scanning electron microscopy (SEM, Hitachi, SU 70). Specific surface area was obtained with a Micrometics apparatus. The absorption gas used was nitrogen, and the measurements are made at 77 °K (Brunauer et al. 1938), using the BET (Brunauer-Emmett-Teller) method. Fourier transform infra-red (FTIR) spectra were obtained with samples in KBr discs using a Perkin Elmer spectrometer (Chaari et al. 2015). The dye used in this present study is methylene blue (MB, Fluka 96%), an aromatic heterocyclic azo compound with the molecular formula $C_{16}H_{18}N_3SCl$.

The effect of parameters such as contact time, solution pH, and initial dye concentration was studied in order to refine and optimise the removal process of methylene blue from laboratory-prepared aqueous solutions, using the previously prepared clay materials.

Adsorption experiments

Adsorption tests of MB were performed in batches at room temperature (25 °C) with varying contact times, and initial MB dye concentrations of 10, 50, 75, 100, 150, and 200 ppm. 0.1 g of adsorbent (H) was added to 100 mL of MB solution. The solutions were mixed vigorously with a mechanical stirrer in the dark to avoid photolysis, and samples were collected at predetermined time intervals of 0, 10, 20, 30, 40, 60, 90, and 120 min. After centrifugation at 4000 rpm for 15 min, the sample solution was analysed by measuring the absorbance at a wavelength of 663 nm, using a Shimadzu UV3100 spectrometer. Batch mode adsorption was selected due to its simplicity and reliability.

The dye removal efficiency was calculated according to:

$$\text{Dye removal efficiency}\ (\%) = \frac{C_i - C_e}{C_i} * 100 \quad (1)$$

$$q_e = \frac{C_i - C_e}{W} * V \quad (2)$$

where C_i and C_e (mg/L) are initial and equilibrium dye concentrations, respectively, q_e (mg/g) is the adsorption capacity, W (g) is the mass of raw clay (H) (g), and V (mL) represents the volume of adsorbate.

The study of adsorption isotherms makes it possible to determine the adsorption capacity of the adsorbates on the adsorbent and the type of adsorption mechanism.

To interpret the adsorption phenomenon of methylene blue on the studied clay, we applied the Langmuir (Langmuir 1918) and Freundlich (Freundlich 1906) models (Eloussaeif et al. 2009; Chaari et al. 2015).

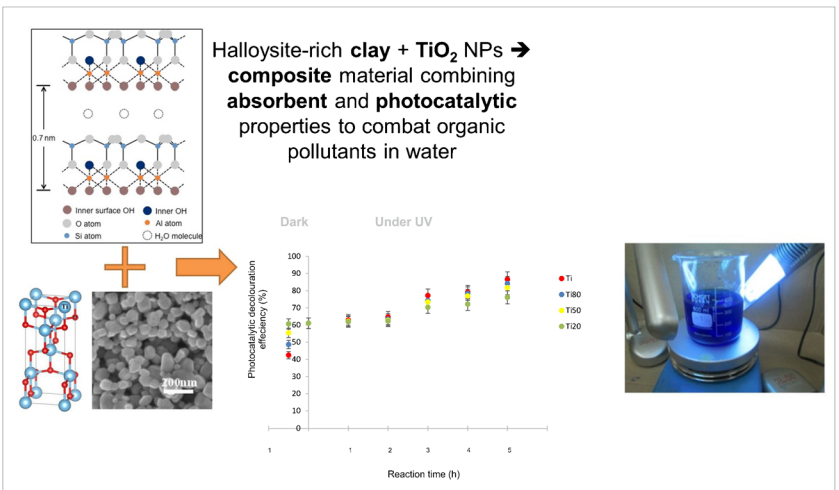

Fig. 1 Photocatalytic experimental setup

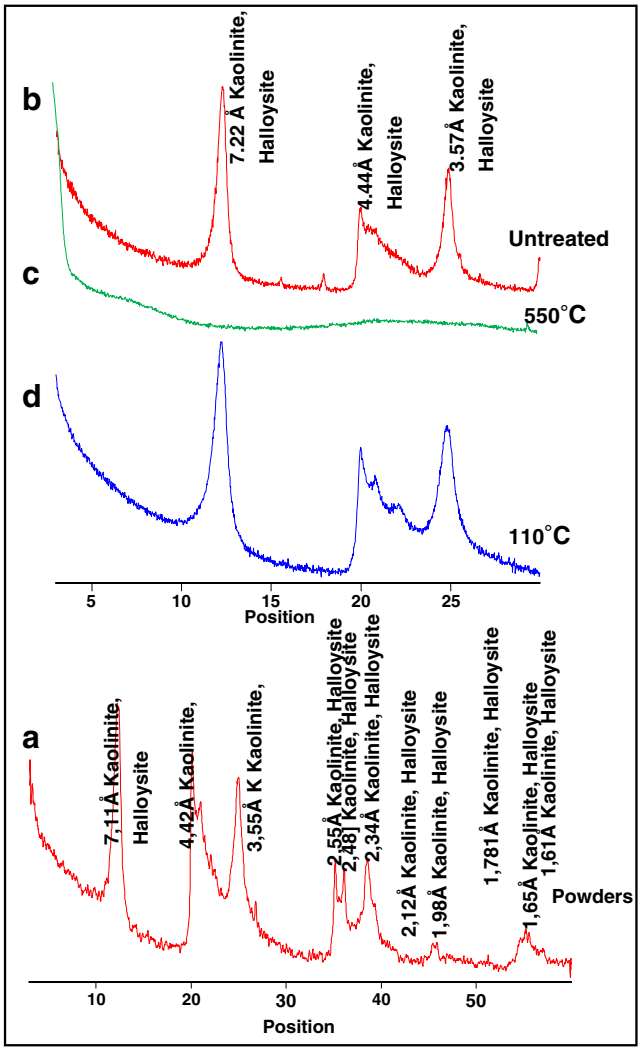

Fig. 2 X-ray diffraction pattern of the powdered clay (a) and the oriented clay fraction (<2 μm) (untreated (b), heated at 550 °C (c), and glycolated (d))

The Langmuir equation is:

$$\frac{t}{q_e} = \frac{1}{q_m} + \frac{1}{K_L q_m C_e} \tag{3}$$

where q_m (mg/g) = maximum capacity of adsorption, q_e (mg/g) = capacity at adsorption equilibrium, K_L (L/mg) = the Langmuir constant, and $1/K_L$ is the slope of the plot. The value of q_m is obtained from the intersection with the ordinate in the beginning, and K_L from the slope of the right-hand side, $C_e/q_e = f(C_e)$.

Table 1 Chemical analysis (%) of the halloysite-rich clay studied. *LOI* loss on ignition

Clay sample	SiO_2	Al_2O_3	Fe_2O_3	CaO	K_2O	TiO_2	P_2O_5	LOI
H	43.6	39.2	0.52	0.10	0.42	0.02	0.03	15.9

The Freundlich equation is:

$$\log q_e = \log K_f + \left(\frac{1}{n}\right) \log C_e \tag{4}$$

where K_f and $1/n$ are constant and considered as indicators of adsorption intensity. The value of $1/n$ is an indication of the validity of adsorbent-adsorbate system. Values of $n > 1$ indicate that the adsorption intensity is favourable (Eloussaeif et al. 2009; Karim et al. 2010; Lazaar et al. 2017).

To know if the Langmuir models are favourable or not towards adsorption occurring, the factor of separation, R_L, is used (Langmuir 1918).

This factor is calculated using the equation (Ašperger et al. 2014):

$$R_L = \frac{1}{1 + K_L C_0} \tag{5}$$

where K_L = the Langmuir constant (L mg^{-1}) and C_0 = initial dye concentration (mg L^{-1}).

The adsorption kinetics were studied using two models, the pseudo-first-order and pseudo-second-order equations.

The pseudo-first order kinetic (Robalds et al. 2016) is expressed as follows:

$$\log(q_e - q_t) = \log q_e - \left(\frac{k_1}{2.303}\right) t \tag{6}$$

where q_e (mg/g) = the amount of MB adsorbed at adsorption equilibrium, q_t (mg/g) = the amount of the MB adsorbed at the time t (min), and k_1 = the equilibrium rate constant (min^{-1}).

The pseudo-second-order model is derived from (Bhattacharyya and Sharma 2004):

$$t/q_t = 1/k_2 q_e^2 + t/q_e \tag{7}$$

where q_e (mg/g) is the capacity at adsorption equilibrium, and k_2 (g mol^{-1} min^{-1}) is the constant speed of adsorption.

where k_2 = the adsorption rate constant, and q_e and q_t are the quantities of MB dye adsorbed at equilibrium and after time t, respectively, in mg/g.

Photocatalytic experiments

A 50 ppm of MB solution was used with 0.25 g of photocatalyst (TiO_2/clay), after mixing the solution for 10 min. The UV irradiation was only triggered after magnetically stirring the suspension for 30 min in the dark, in order to obtain an adsorption equilibrium. The UVA-light source was a germicidal lamp (Philips PL-S 9 W), with an irradiance of approximately 13 W m^{-2}. The UV exposure was carried out using two lamps on either side of the reactor (Fig. 1), with a

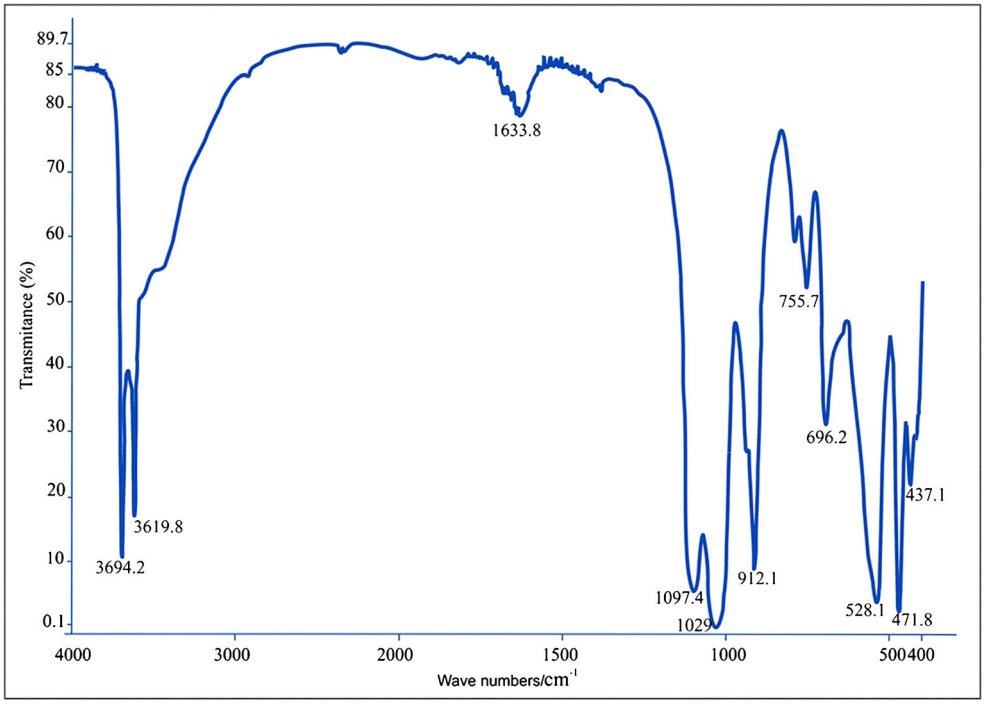

Fig. 3 FT-IR spectrum of the raw clay (H)

distance of 5 cm between the lamps and the reactor (Hajjaji et al. 2016).

The substrate removal rate (R) was calculated using the following relationship:

$$R\,(\%) = \frac{C_0 - C_t}{C_0} * 100 \quad (8)$$

where C_0 (mg/L) = initial dye concentration, and C_t (mg/L) = its concentration after a certain UV irradiation time.

The apparent speed constant (k'_{app}) was calculated from the pseudo first-order reaction as follows:

$$\ln (C_0/C) = k'_{app}\, t \quad (9)$$

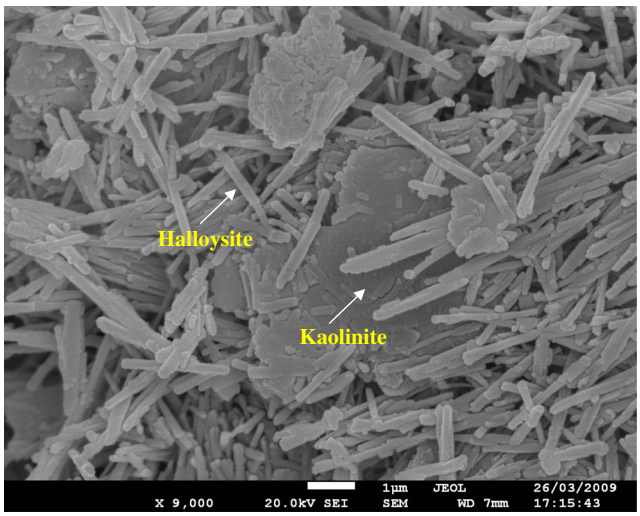

Fig. 4 SEM images of the raw clay (H)

where C_0 = initial dye concentration, and C = its concentration after irradiation time t. The plot of ln (C_0/C) vs the contact time t under UV exposure gives a straight line, where the slope corresponds to the apparent pseudo-first-order rate constant (k'_{app}) (Hajjaji et al. 2016).

Results and discussion

Characterisation of the raw clay

The XRD of the raw clay shows the presence of halloysite (H) (61%) associated with kaolinite (K) (39%) (Fig. 2). Table 1 also gives the X-ray fluorescence chemical composition of the clay sample. This analysis showed a dominance of SiO_2 (43.6%) and Al_2O_3 (39.2%). Relatively low contents of Na_2O and K_2O were also identified. Figure 3 shows the FT-IR spectrum of the raw clay (H). This spectrum shows absorption bands between 3694 and 917 cm^{-1}, attributable to Al-Al-OH^- stretching and bending vibration modes. According to the literature (Moussi et al. 2011), halloysite is chemically similar to kaolinite. On other hand, the hydrated form of

Table 2 Specific surface area, pore volume, and average pore diameter of used clay, as determined by BET

Clay material	S_{BET} (m^2/g)	Pore volume (cm^3/g)	Pore diameter (Å)
H	43.57	0.0015	181.38

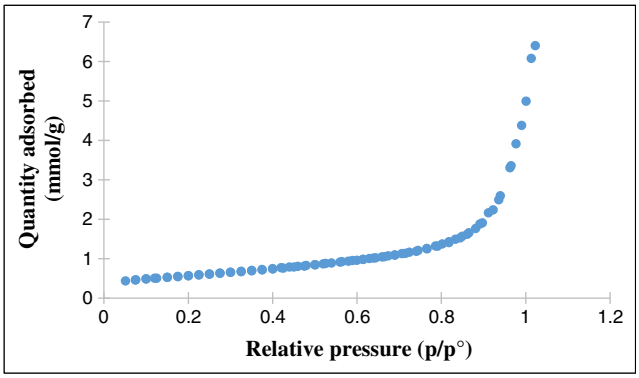

Fig. 5 Nitrogen adsorption isotherms for the raw clay (H)

halloysite, named "halloysite - (10 Å)", has one layer of water molecules sandwiched between the multilayers (Yuan et al. 2015). SEM (Fig. 4) showed that our material was composed of a halloysite phase, with a tubular structure typical of hydrated halloysite and kaolinite in platy form.

The BET-specific surface area (SSA) of the clay (H) is presented in Table 2. The values of the SSA of the material were 43.57 m^2/g. The N_2 adsorption–desorption isotherms of the clay are shown in Fig. 5, and they have a type IV adsorption isotherm, indicating that our clay is a mesoporous material, with the pore diameter exceeding 20 Å (Webb and Orr 1988). The measured BET pore diameter of the clay was 181 Å.

Adsorption experiments

MB adsorption performance

These tests were applied to raw clay (H). The influence of time on the adsorbed quantity (Fig. 6) is considered as an important factor in this solid (H)-liquid (MB) extraction process. Indeed,

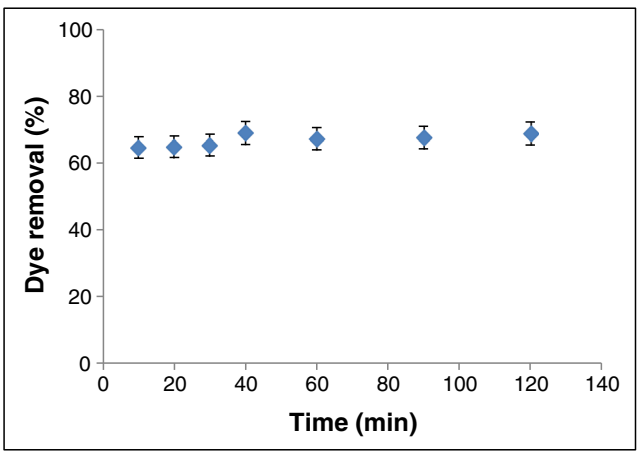

Fig. 6 Adsorption kinetics: effect of contact time of clay (H) on subsequent adsorption of MB. Experimental conditions: $C_i = 50$ ppm; $T = 25$ °C; $m_{adsorbent} = 0.1$ g

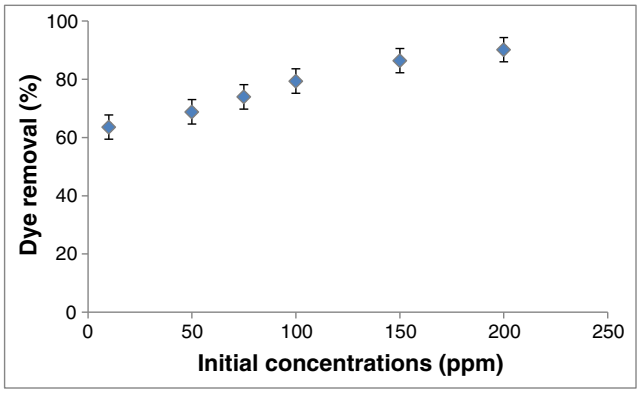

Fig. 7 Adsorption kinetics: effect of initial concentration of MB in dye solution on adsorption of MB. Experimental conditions: $T = 25$ °C; $m_{adsorbent} = 0.01$ g; time of equilibrium = 120 min

it helps to determine the equilibrium time of the reaction and the kinetics of adsorption. The clay showed a very rapid initial adsorption of MB (50 ppm), with 64.7% adsorbed after only 10 min. After 120 min of reaction time, the discoloration rate had only increased to 68.8%, and the results indicate that an equilibrium was obtained after only 60 min. The effect of the initial MB concentration is shown in Fig. 7. The results show that, when increasing the initial dye concentration, the absorption capacity of the clay increases, reaching up to 90% when the initial MB concentration was 200 ppm. These values for absorption capacity are close to those reported by Hajjaji et al. (2013) and Andolsi (2016) in studies on the kinetics of MB adsorption by clay. In this case, the initial concentration provided the driving force needed to overcome the mass transfer resistance of MB between the clay's aqueous and solid phases (Ouasif et al. 2013; Mahammadi and Benguella 2016).

Equilibrium and kinetics of MB adsorption

To interpret the adsorption phenomenon of methylene blue on the studied clay, we applied the Freundlich and Langmuir models, the experimental Freundlich and Langmuir isotherms of the clay being shown in Fig. 8, using 50 ppm of MB. The values of the constants corresponding to each model are summarised in Table 3. The maximum adsorption capacity, determined from the Langmuir monolayer isotherm, is 31.25 mg/g for the raw clay. It was considered that this natural clay has a moderate adsorption capacity in comparison with other raw clays reported in literature (Hajjaji et al. 2013). The high coefficient of determination ($R^2 = 0.96$) confirmed that these experimental data fit the Langmuir model well. These results also showed that that R_L was >0, indicating a favourable adsorption of MB using this clay.

The measured parameters K_f and n by the Freundlich model, summarised in Table 3 and in Fig. 8, also indicated that the adsorption process was favourable ($0 < 1/n < 1$), and there were higher probabilities of multilayer adsorption of MB

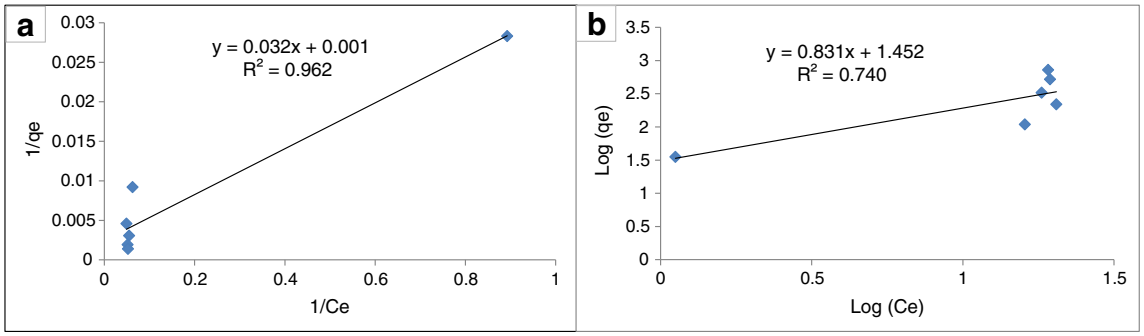

Fig. 8 Fitting with the linear Langmuir (a) and Freundlich (b) models for MB adsorption on clay (H)

molecules through a percolation mechanism on the active surface sites. However, the smaller R^2 ($R^2 = 0.74$) regression coefficient indicated a lesser affinity for interaction between the adsorbate–adsorbent in this case. This demonstrates that a monolayer adsorption, as depicted by the Langmuir model, with a heterogeneous energetic distribution of the active sites is more likely, accompanied by interactions between the adsorbed molecules (Hajjaji et al. 2013; Lazaar et al. 2017). Therefore, the values of the constants of each model (Table 3) indicate that the Langmuir model perfectly represents the adsorption process of MB, with a correlation coefficient value close to unity (0.96), and the value of the Langmuir separation factor (R_L) is in the range of validity (between 0 and 1). This reinforces the reliability of the Langmuir model, which relies on the absence of interactions between the entities adsorbed on sites of the same nature (Laabd et al. 2015).

The kinetics of MB adsorption on the clay were better described by a pseudo-second-order equation than a pseudo-first-order one. There was a much better fit of the pseudo-second-order equation, which had an average regression coefficient of $R^2 = 0.997$, compared to $R^2 = 0.78$ for the pseudo-first-order model. These results suggested that the removal process is due to chemisorption (Kooli et al. 2015). Moreover, the q_e value obtained experimentally using a pseudo-second-order kinetic model (26.31 mg/g) was close to the calculated adsorption capacity at equilibrium from the Langmuir isotherm (31.25 mg/g) (Table 4). This model is in good agreement with other MB adsorption on clay reported in recent articles. These values of q_e are close to those reported by Andolssi (2016) and Chargui et al. (2018) in their studies on the kinetics of MB adsorption by clay.

Photocatalytic decolouration of MB

It is important to state that the photoactivity test was carried out by comparing the photocatalytic removal efficiency in the presence of the mixed clay-TiO_2 material under UV irradiation with the amount of adsorption in the dark. These TiO_2 nanoparticles will absorb UV light to give rise to very reactive oxygen species (ROS), which will lead to the degradation of the substance in solution (Ammari et al. 2016). The removal rates of the MB dye solutions by clay/titania P25 composites, initially in the dark for 30 min, and then under UV irradiation for 3 h of reaction, are shown in Table 5 and in Fig. 9. From all these results, we find that during the initial 30 min without UV light exposure, adsorption of the MB solution increases with a decrease in the proportion of P25 titania in the clay (42.4% and 60.6% of removal for Ti and Ti20, respectively). This could be explained by the decrease of the porosity of the clay by increasing the charge of the TiO_2 aggregates in the interfoliar space, which leads to the reduction of the active sites for the adsorption of the MB molecules (Djellabi 2015), as well as there being a lower wt% of the clay present as TiO_2 levels increase. These results also explain the low value of the R^2 coefficient for decolouration observed in the Ti50 sample, ($R^2 = 0.59$), as it contains a less than optimum amount of either clay or TiO_2 at 50 wt% of each. By comparison, the R^2 values for Ti80 and Ti20 are virtually identical, at 0.80 and 0.79, respectively (Table 5). Under UV irradiation, all the clays with different ratios of TiO_2 (Ti80, Ti50, and Ti20) show slower MB photodecolouration than the pure P25 powder

Table 3 Langmuir and Freundlich parameters for MB adsorption on studied sample (H), estimated at room temperature

Material	Langmuir			Freundlich		
	q_m (mg/g)	R_L	R^2	K_f (L/g)	n	R^2
H	31.25	0.003	0.96	3.95	1.20	0.74

Table 4 Pseudo-first- and second-order parameters for MB adsorption

Material	Pseudo-first-order				Pseudo-second-order		
	k_1 (min^{-1})	q_e (mg/g)	R^2	q_e (exp)	k_2 (g/mg min)	q_e (mg/g)	R^2
H	−0.1	80.26	0.78	36.98	0.038	26.31	0.997

Table 5 Photocatalytic decolouration efficiency (ξ) and correlation coefficient (R^2) of the pseudo-first-order apparent constant of the photocatalytic reaction (Ti = 100% TiO_2)

	R^2				ξ (%)			
	Ti	Ti80	Ti50	Ti20	Ti	Ti80	Ti50	Ti20
H	0.85	0.80	0.59	0.79	86.6	84.1	81.7	76.1

(Ti), with all samples reaching their maximum degradation only after 3 h of UV irradiation (Fig. 9). Nevertheless, the clay-TiO_2 composites exhibited a photocatalytic efficiency only slightly lower than that of the pure TiO_2 powder, with values of 86.6%, 84.1%, 81.7%, and 76.1% for Ti, Ti80, Ti50, and Ti20, respectively.

Therefore, we can see that the clay-TiO_2 mixture successfully combines the phenomena of adsorption and photocatalysis, with little loss in photocatalytic decolouring efficiency, while maintaining a strong ability to physically adsorb MB.

The plot of $\ln(C_0/C)$ versus t with different mixtures of clay (H)/TiO_2 is shown in the Table 6 and Fig. 10. All the curves showed a good linear correlation ($R^2 > 0.90$), suggesting that the decolouration of MB by clay-TiO_2 with UV light followed a first-order kinetic.

Under the same experimental conditions, the apparent rate constant (k'_{app}) of MB decolouration was 0.313, 0.292, 0.247, and 0.201 min^{-1}, when the percentage (wt%) of TiO_2 used was 100, 80, 50, and 20, respectively. As the mass of TiO_2 decreases, the apparent rate constant of photodecolouration decreases, as would be expected.

Table 6 The apparent rate constant of the photocatalytic reaction as a function of the percentage of TiO_2

TiO_2 (%)	100	80	50	20
k'_{app} (min^{-1})	0.313	0.292	0.247	0.201

The pH of the aqueous solution is one of the most important factors in controlling the adsorption process, and its effect on photocatalytic activity is important in order to evaluate the efficiency of the technique, in this case for water loaded with a pollutant. To evaluate the effect of pH on the adsorption phenomenon, the adsorption of MB dye with pH values of 3, 7, and 10 was studied. The photocatalytic decolouration of MB is best at acidic pH for pure P25 powder, the maximum decolouration of this dye being observed at pH = 3 (98% photocatalytic decolouration efficiency for Ti and Ti80). Indeed, in an acidic medium, strong adsorption of the dye on the TiO_2 nanoparticles and clays is observed, probably due to the electrostatic attraction between the positive charge of TiO_2/clays and the negative charge of the dye. However, the rate of photocatalytic decolouration decreases with increasing pH (> 7). We observed 95% and 83% photocatalytic decolouration efficiency for Ti and Ti80, respectively, at pH 7, and 90% and 81% photocatalytic decolouration efficiency for Ti and Ti80, respectively, at pH 10.

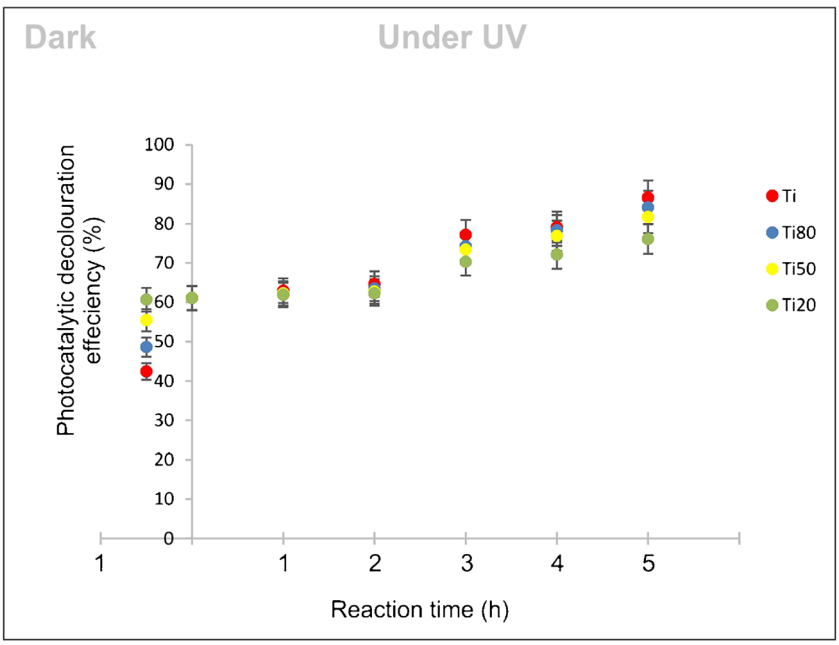

Fig. 9 Photocatalytic removal kinetics of 50-ppm MB dye under UV light by clay (H)-based titania/clay composites

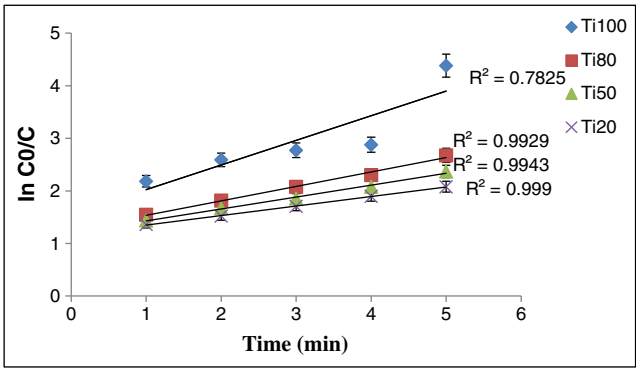

Fig. 10 Photocatalytic rate constants as a function of the different amounts of TiO_2/clay, using a 50-ppm MB solution

Conclusions

This work reports the use of a Tunisian clay containing several phases, namely halloysite and kaolinite, in the removal of methylene blue cationic dye.

For methylene blue adsorption, the pure clay material presented a lower adsorption capacity. The clay removed 68% of a 50-ppm methylene blue solution removal by adsorption after only 2 h, and at a concentration of 200 ppm, the adsorption capacity reached 90%. Fitting of experimental values by the Langmuir isotherm model parameters was very acceptable (R^2 up to 0.96), which reveals that the adsorption process corresponds to a monolayer coverage of MB molecules.

The second part reports the use of a constant quantity of different mixtures of clay/P25 TiO_2, with 0, 20, 50, and 80 wt% TiO_2 added to endow photocatalytic properties. With 20 wt% added TiO_2 photocatalyst, this gave ~60% removal after 1 h, increasing to 84.1% removal after a further 3 h under UV light, through combined chemo-physical adsorption and photocatalytic decolouration phenomena. Due to the combined effects of adsorption and photocatalysis, the removal of methylene blue from the solutions was very efficient, even with clay compositions containing low TiO_2 levels. The photocatalytic decolouration efficiency was influenced by the change in pH. At an acidic pH of 3, high dye removal efficiency was obtained (98% removal after 300 min). The high dye removal efficiency at low pH is due to the electrostatic attraction between the negatively charged dye and the positively charged adsorbent surface.

Funding This study was supported by funding from MEDYNA: "FP7-Marie Curie Action funded under Grant Agreement PIRSES-GA- 2013-612572". Robert C. Pullar acknowledges the support of the Fundação para a Ciência e Tecnologia (FCT) grant IF/00681/2015. This work was developed within the scope of the project CICECO-Aveiro Institute of Materials, UIDB/50011/2020 & UIDP/50011/2020, financed by national funds through the FCT/MEC and when appropriate co-financed by FEDER under the PT2020 Partnership Agreement.

Compliance with ethical standards

Conflict of interest The authors declare no competing interests.

References

Ahmadkhan S, Arshad Z, Shahid S, Arshad I, Rizwan K, Sher M, Fatima U (2019) Synthesis of TiO_2/Graphene oxide nanocomposites for their enhanced photocatalytic activity against methylene blue dye and ciprofloxacin. Comp Part B 175:107–120

Alahiane S, Qourzal S, El Ouardi M, Belmouden M, Assabbane A, Ait-Ichou Y (2013) Adsorption et photodégradation du colorant indigo carmine en milieu aqueux en présence de TiO2/UV/O2 (Adsorption and photocatalytic degradation of indigo carmine dye in aqueous solutions using TiO2/UV/O2). J Mater Environ Sci 4:239–250

Aloulou W, Hamza W, Aloulou H, Oun A, Khemakhem S, Jada A, Chakraborty S, Curcio S, Ben Amar R (2018) Developing of titania-smectite nanocomposites UF membrane over zeolite based ceramic support. Appl Clay Sci 155:20–29

Ammari Y, Elatmani K, Qourzal S, Bakas I, Ejakouk E, Ait-Ichou Y (2016) Etude cinétique de la dégradation photocatalytique du colorant bleu de méthylène en présence de dioxyde de titane (TiO2), en suspension aqueuse (Kinetic study of the photocatalytic degradation of methylene blue dye in the presence of titanium dioxide (TiO2), in aqueous suspension). J Mater Environ Sci 7:671–678

Andolsi A (2016) Utilisation d'une argile kaolinitique dans l'élimination du bleu de méthylène: adsorption et oxydation avancée. Mémoire de Mastère. ISSTE, Borj Cédria, Tunisie, 58 pp.

Annadurai G, Juang RS, Lee DJ (2002) Use of cellulose-based wastes for adsorption of dyes from aqueous solution. J Hazard Mater B 92: 263–274. https://doi.org/10.1016/S0304-3894(02)00017-1

Arana J, Melian JAH, Rodriguez JM, Diaz DOG, Viera A, Pena JP, Sosa PM, Jimenez VE (2002) TiO2-photocatalysis as a tertiary treatment of naturally treated wastewater. Catal Today 76:279–289

Asefi N, Masoudpanah M, Hasheminiasari M (2019) Photocatalytic performances of $BiFeO_3$ powders synthesized by solution combustion method: the role of mixed fuels. Mater Chem Phys 228:168–174

Ašperger D, Varga I, Babić S, Ćurković L (2014) Adsorption of enrofloxacine on natural zeolite –clinoptilolite. Holistic Approach Environ 4:3–15

Ben Amor T, Kassem M, Hajjaji W, Jamoussi F, Ben Amor M, Hafiane A (2018) Study of defluoridation of water using natural clay minerals. Clay Clay Miner 66:493–499

Bhattacharjee S, Chakraborty S, Mandol K, Liu L, Choi H & Bhattacharjee C (2014) Optimization of process parameters during photocatalytic degradation of phenol in UV annular reactor. Desalin Water Treat 1–10. https://doi.org/10.1080/19443994.2014.896750

Bhattacharya J, Choudhary U, Biwach O, Sen P, Dasgupta-Nanomed A (2006) Nanotechnol. Biol Med 2:191–199

Brunauer S, Emmett PH, Teller EJ (1938) Adsorption of gases on multimolecular layers. J Am Chem Soc 60:309–319

Chaari I, Fakhfakh E, Chakroun S, Bouzid J, Boujelben N, Feki M, Rocha F, Jamoussi F (2008) Lead removal from aqueous solutions by a Tunisian smectitic clay. J Hazard Mater 156:545–551

Chaari I, Moussi B, Jamoussi F (2015) Interactions of the dye, C.I. direct orange 34 with natural clay. J Alloys Compd 647:720–727

Chakraborty S, Rusli H, Nath A, Sikder J, Bhattacharjee C, Curcio S, & Drioli E (2014) Immobilized biocatalytic process development and potential application in membrane separation: a review. Crit Rev Biotechnol, Early Online: 1–16

Chakraborty S, Loutatidou S, Palmisano G, Kujawa J, Mavukkandy MO, Al-Gharabli S, Curcio E, Arafat HA (2017) Photocatalytic hollow fiber membranes for the degradation of pharmaceutical compounds

in wastewater. J Environ Chem Eng 5:5014. https://doi.org/10.1016/j.jece.2017.09.038
Chargui H, Hajjaji W, Wouters J, Yans J, Jamoussi F (2018) Direct Orange 34 dye fixation by modified kaolin. Clay Miner 53:1–32
Crini G (2006) Non-conventional low-cost adsorbentsfor dyes removal: a review. Bioresour Technol 97:1061–1085
Das L, Basu JK (2014) Photocatalytic treatment of textile effluent using titania–zirconia nano composite catalyst. J Ind Eng Chem 2232:1–6
Das R, Sarkar S, Chakraborty S, Choi H, Bhattacharjee C (2014) Remediation of antiseptic components in wastewater by photocatalysis using TiO_2 nanoparticles. Ind Eng Chem Res 53: 3012–3020
Djellabi R (2015) Contribution de la photocatalyse à l'élimination des polluants industriels. PhD thesis, university of Badji Mokhtar – Annaba, Algérie, 168 pp.
Dogan M, Alkan M (2003) Adsorption kinetics of methylviolet onto perlite. Chemosphere 50:517–528
Eloussaief M, Jarraya I, Benzina M (2009) Adsorption of copper ions on two clays from Tunisia: pH and temperature effects. Appl Clay Sci 46:409–413
Freundlich HMF (1906) Over the adsorption in solution. Z Phys Chem 57:385–471
Gong Y, Li M, Li H, Wang Y (2015) Graphitic carbon nitride polymers: promising catalysts or catalyst supports for heterogeneous oxidation and hydrogenation. Green Chem 2:1–53
Hajjaji W (2011) Valorisation des sables siliceux et des argiles du cretace inferieur de la tunisie centrale et meridionale. Thèse de doctorat. Fac. Sc. Bizerte, Tunisia, 120 pp.
Hajjaji W, Ganiyu SO, Tobaldi DM, Andrejkovičová S, Pullar RC, Rocha F, Labrincha JA (2013) Natural Portuguese clayey materials and derived TiO_2-containing composites used for decolouring methylene blue (MB) and orange II (OII) solutions. Appl Clay Sci 83:91–98
Hajjaji W, Andrejkovičová S, Pullar RC, Tobaldi DM (2016) Effective removal of anionic and cationic dyes by kaolinite and TiO_2/kaolinite composites. Clay Miner 51:19–27
Karim AB, Mounir B, Hachkar M, Bakasse M, Yaacoubi A (2010) Removal of basic dye "methylene blue" in aqueous solution by Safi clay. J Water Sci 23:375–388
Kooli F, Yan L, Al-Faze R, Al-Sehimi A (2015) Removal enhancement of basic blue 41 by brick waste from an aqueous solution. Arab J Chem 8:333–342
Laabd M, EL-Jaouhari A, Chafai H, Aarab N, Bazzaoui M, Albourine A (2015) Etude cinétique et thermodynamique de l'adsorption des colorants monoazoïques sur la polyaniline. J Mater Environ Sci 6: 1049–1059
Langmuir I (1918) The adsorption of gases on plane surfaces of glass, mica and platinum. J Am Chem Soc 40:1361–1403
Lazaar K, Hajjaji W, Pullar RC, Labrincha JA, Rocha F, Jamoussi F (2017) Production of silica gel from Tunisian sands and its adsorptive properties. J Afr Earth Sci 130:238–251
Mahammedi F, Benguella B (2016) Adsorption of methylene blue from aqueous solutions using natural clay. J Mater Environ Sci 7:285–292
Meshko V, Markovska L, Mincheva M, Rodrigues AE (2001) Adsorption of basic dyes on granular activated carbon and natural zeolite. Water Res 35:3357–3366
Mokhbi Y, Korichi M, Sidrouhou HM, Chaouche K (2014) Treatment heterogeneous photocatalysis; factors influencing the photocatalytic degradation by TiO2. Energy Procedia 50:559–566
Moussi B, Medhioub M, Hatira N, Yans J, Hajjaji W, Rocha F, Labrincha J.A & Jamoussi F (2011) Identification and use of white clayey deposits from the area of Tamra (northern Tunisia) as ceramic raw materials. Clay Miner 46:165–175
Mudzielwana R, Gitari MW, Ndungu P (2019) Uptake of As(V) from groundwater using Fe-Mn oxides modified kaolin clay: physico-chemical characterization and adsorption data modeling. Water 11: 1245
Mustapha S, Ndamisto MM, Abdulkreem AS, Tijani JO, Shuaib DT, Ajala AO, Mohammed AK (2020) Application of TiO2 and ZnO nanoparticles immobilized on clay in wastewater treatment: a review. Appl Water Sci 10:49
Naidoo S & Olaniran A (2014) Treated wastewater effluent as a source of microbial pollution of surface water resources. Int. J. Environ. Res. Public Health 11:249–270
Ngoh YS, Nawi MA (2016) Role of bentonite adsorbent sub-layer in the photocatalyticadsorptive removal of methylene blue by the immobilized TiO/bentonite system. Int J Environ Sci Technol 13: 907–926
Ouasif H, Yousfi S, Bouamrani ML, El Kouali M, Benmokhtar S, Talbi M (2013) Removal of a cationic dye from wastewater by adsorption onto natural adsorbents. J Mater Environ Sci 4:1–10
Priya R, Stanly S, Kavitharani T, Mohammad F, Sagadevan S (2020) Highly effective photocatalytic degradation of methylene blue using PrO2–MgO nanocomposites under UV light. Optik – Int J Light Electron Optics 206:164318. https://doi.org/10.1016/j.ijleo.2020.164318
Robalds A, Dreijalte L, Bikovens O, Klavins M (2016) A novel peat-based biosorbent for the removal of phosphate from synthetic and real wastewater and possible utilization of spent sorbent in land application. Desalin Water Treat 57:13285–13294
Sakr F, Sennaoui A, Elouardi M, Tamimi M, Assabbane A (2015) Étude de l'adsorption du Bleu de Méthylène sur unbiomatériau à base de Cactus (Adsorption study of Methylene Blue on biomaterial using cactus). J Mater Environ Sci 6:397–406
Sarkar S, Sondhi K, Das R, Chakraborty S, Choi H, Bhattacharjee C (2015) Development of a mathematical model to predict different parameters during pharmaceutical wastewater treatment using TiO2 coated membrane. Ecotoxicol Environ Saf 121. https://doi.org/10.1016/j.ecoenv.2015.03.041
Sdiri T, Higashi T, Jamoussi F (2014) Adsorption of copper and zinc onto natural clay in single and binary systems. Int J Environ Sci Technol 11:1081–1092
Tobaldi DM, Pullar RC, Seabra MP, Labrincha JA (2014) Fully quantitative X-ray characterisation of Evonik Aeroxide TiO_2 P25. Mater Lett 122:345–347
Tunç I.D, Erol M, Güneş F & Sütçü M (2019) Growth of ZnO nanowires on carbon fibers for photocatalytic degradation of methylene blue aqueous solutions: an investigation on the optimization of processing parameters through response surface methodology/central composite design. Ceramics International. https://doi.org/10.1016/j.ceramint.2019.11.244
Webb P, Orr C (1988) Analytical methods in fine particle technology. Micromeritics Instrument Corporation, Norcross
Weber R, Watson A, Forter M, Oliaei F (2011) Review article: Persistent organic pollutants and landfills - a review of past experiences and future challenges. Waste Manag Res 29:107–121
Wongso V, Chen CJ, Razzaq A, Kamal NA (2019) Hybrid kaolin/TiO2 composite: effect of urea addition towards an efficient photocatalyst for dye abatement under visible light irradiation. Appl Clay Sci 180: 105158
Yuan P, Tan D, Annabi-Bergaya F (2015) Properties and applications of halloysite nanotubes: recent research advances and future prospects. Appl Clay Sci 112:75–93
Yu-Li YR, Thomas A (1995) Colour removal from dye wastewaters by adsorption using powdered activated carbon: mass transfer studies. J Chem Technol Biotechnol 63:48–54